The Journal of Experimental Biology 214, 2871-2882

doi:10.1242/jeb.055582

RESEARCH ARTICLE

Sheep rumen and omasum primary cultures and source epithelia: barrier function aligns with expression of tight junction proteins

Friederike Stumpff[1,*], Maria-Ifigenia Georgi[1], Lars Mundhenk[2], Imtiaz Rabbani[1,3], Michael Fromm[4], Holger Martens[1] and Dorothee Günzel[4]

[1]Department of Veterinary Physiology, Freie Universität Berlin, 14163 Berlin, Germany, [2]Department of Veterinary Pathology, Freie Universität Berlin, 14163 Berlin, Germany, [3]Department of Clinical Medicine and Surgery, University of Veterinary and Animal Sciences, Lahore 54000, Pakistan and [4]Institute of Clinical Physiology, Charité Berlin, Campus Benjamin Franklin, 12200 Berlin, Germany

*Author for correspondence (stumpff@zedat.fu-berlin.de)

Accepted 25 May 2011

SUMMARY

The forestomachs of cows and sheep have historically served as important models for the study of epithelial transport. Thus, the ruminal epithelium was among the first tissues in which absorption of chloride against an electrochemical gradient was observed, requiring a tight paracellular barrier to prevent back-leakage. However, little is known about ruminal barrier function, despite the considerable implications for ruminant health. The tight junction proteins of the omasum have never been investigated, and no cell culture model exists. We present a new method for the isolation of cells from forestomach epithelia. Protein expression of cells and source tissues of sheep were studied using western blot, PCR and confocal laser scanning microscopy. Cultured cells were characterized by transepithelial resistance (TER) measurements and patch clamping. Cells developed TER values of 729±134 Ω cm^2 (rumen) and 1522±126 Ω cm^2 (omasum). Both primary cells and source epithelia of rumen and omasum expressed cytokeratin, occludin and claudins 1, 4 and 7 (but not claudins 2, 3, 5, 8 and 10), consistent with the observed paracellular sealing properties. Staining for claudin-1 reached the stratum basale. The full mRNA coding sequence of claudins 1, 4 and 7 (sheep) was obtained. Patch-clamp analyses of isolated cells proved expression of an anion conductance with a permeability sequence of gluconate<acetate<chloride. This is in accordance with a model that ruminal and omasal transport of anions such as chloride and acetate has to occur *via* a transcellular route and involves channel-mediated basolateral efflux, driven by Na^+/K^+-ATPase.

Supplementary material available online at http://jeb.biologists.org/cgi/content/full/214/17/2871/DC1

Key words: rumen, omasum, barrier, tight junction, claudin, SCFA, VFA, acetate, anion channel, chloride channel, epithelial transport, ruminant.

INTRODUCTION

In studying transport across the forestomachs of ruminants, the economic interest in gaining a better understanding of the digestive tract of these animals converges with the interest of the natural scientist, who seeks a model tissue well suited for the study of epithelial transport *in vivo* and *in vitro*. Unlike the complex anatomy of the glandular tissues of the gastrointestinal tract, forestomach tissues are covered by stratified squamous epithelium (Graham and Simmons, 2005) and thus differentiate from the relatively homogenous cells of the stratum basale, which greatly facilitates the establishment of a suitable cell culture model. The forestomachs thus appear to be ideal tissues for the comparative study of epithelial transport on the level of the animal, the tissue and the cell.

In ruminants, the glandular stomach, or abomasum, is preceded by the three forestomachs, which have evolved from the esophagus (Mutoh and Wakuri, 1989). The rumen forms a fermentation vat in which resident microbials break up ingested matter, producing energy-rich short-chain fatty acids (SCFA, also referred to as volatile fatty acids, VFA) from cellulose, which are absorbed before the ingesta reach the abomasum (which corresponds to the glandular stomach of monogastic species). It is estimated that up to 100 mol day^{-1} of SCFA are produced within and absorbed across the forestomachs of cows (Allen, 1997).

The omasum (or 'bible') was the first forestomach for which an absorptive function was postulated (Colin, 1856), a suggestion undoubtedly inspired by the anatomy of the organ, with multiple leaflets organized in the manner of a book. *In vivo* and *in vitro* data support an extensive role for the omasum in the absorption of Na^+, SCFA and accompanying water from the digesta (Masson and Philipson, 1952; Edrise et al., 1986; Ali et al., 2006). However, related to its greater size (~16 l in sheep and >100 l in cows) and easier accessibility for *in vivo* studies, the rumen has historically received greater attention and the tissue has played a pivotal role in studying the epithelial transport of SCFA (Phillipson and McAnnally, 1942; Aschenbach et al., 2009; Stumpff et al., 2009), chloride (Sperber and Hyden, 1952), ammonia (McDonald, 1948), urea (Decker et al., 1961; Harmeyer et al., 1973; Abdoun et al., 2010), Na^+ (Dobson, 1959) and Mg^{2+} (Martens and Harmeyer, 1978), large quantities of which are physiologically absorbed.

Remarkably little information is currently available about the manner in which the forestomachs maintain a barrier between the ingesta and the blood stream. Large gradients for chloride and sodium (usually blood>rumen) and for potassium, protons and SCFA (usually rumen>blood) are maintained by forestomach epithelia (Leonhard-Marek et al., 2010), requiring a tight paracellular pathway. Correspondingly, a number of pathologies found in the

ruminant involve a breakdown of ruminal barrier function. Thus, large economic losses are related to a condition in which fermentational processes in the rumen lead to an accumulation of SCFA coupled with a decreased ruminal pH (below 5.5) (Plaizier et al., 2008). The condition is associated with rumenitis and multiple systemic manifestations such as liver abscesses, septic emboli and immunological complications. Both a destruction of cells and a loosening of the cellular junctions are discussed.

Although the presence of tight junctions in the rumen and the omasum has long been known (Schnorr and Wille, 1972; Scott et al., 1972), a systematic characterization is long overdue. This study attempts to partially fill this gap. In addition, a method suitable for the selective isolation of epithelial cells from the omasum is presented. The functional expression of tight junction proteins by forestomach cells in culture is demonstrated and supports an epithelial origin of the cells. Finally, and as previously shown for cultured cells of the ruminal epithelium (Stumpff et al., 2009), we show that omasal cells express an anion conductance permeable to acetate that may resolve the question of how this nutrient is absorbed across the basolateral membrane. In summary, we introduce an epithelial cell culture model for permeation studies that may serve as a starting point for comparative investigations of ruminal and omasal transport and barrier function on the level of the tissue and the cell.

MATERIALS AND METHODS

Ethical approval

Sheep were stunned by captive bolt and killed by exsanguination (permit no. T0064/99). The tissues of interest (rumen or omasum) were removed immediately after slaughter and transported to the laboratory in ice-cold phosphate buffered saline (PBS) buffer (Biochrom AG, Berlin, Germany). All experiments were performed according to German laws for the protection of animals.

Isolation of cells from forestomach epithelia

Within a 2 h period after slaughter, tissues were clamped into a purpose-built Ussing-chamber-style device with the apical side facing upward (see Fig. 1A). This device consisted of two polyethylene plates with holes in the middle (diameter 2 cm), between which the tissue could be placed. A piece of polyethylene tubing with a diameter of 3.5 cm was adjoined to the upper plate, serving as the apical chamber. Both sides of the tissue were superfused with Ca^{2+}- and Mg^{2+}-free DPBS buffer solution (Dulbecco's PBS + EDTA + 4% penicillin/streptomycin; 10,000 U ml^{-1}/10,000 µg ml^{-1}; Biochrom AG, Berlin, Germany) to which trypsin-EDTA (final concentration 0.25%; Sigma-Aldrich, St Louis, MO, USA) was added apically in order to detach the epithelial cell layers from the tissue (at 37°C in a shaking warm-water bath). Care was taken to ensure equal hydrostatic pressure on both sides of the epithelium by adding appropriate amounts of buffer to both sides. The apical supernatant with dissected cells (approximately 25 ml for an epithelial surface of ~3 cm^2) was harvested roughly every 30 min and replaced with fresh buffer. Repeated, forceful ejection and reaspiration of the trypsin solution onto the epithelium further promoted dissociation of cells from the epithelium.

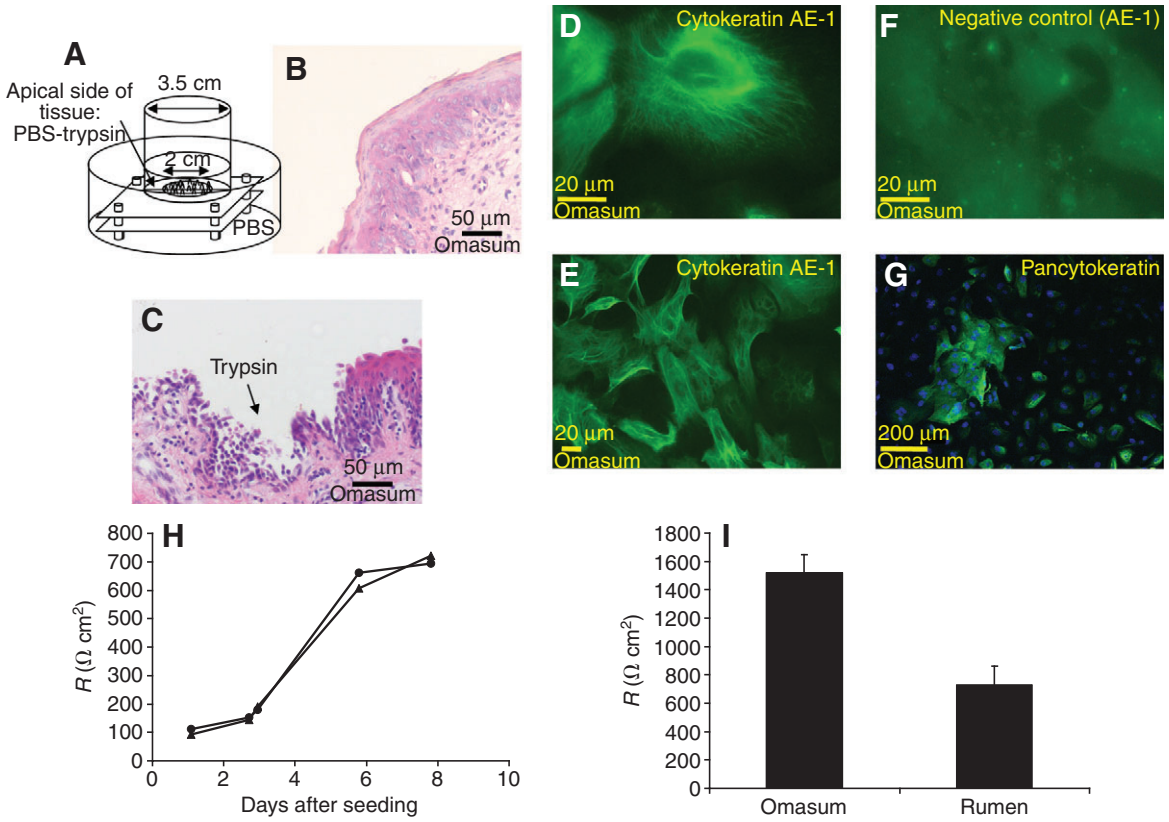

Fig. 1. An improved method for the isolation of cells from sheep forestomach epithelia. (A) Representation of the device used for the incubation of the tissue (see text for details). (B) Hematoxylin & Eosin (H&E) staining of intact tissue of the omasum. (C) Omasal tissue after treatment with trypsin. (D,E) Staining of the cultured cells for cytokeratin AE-1. (F) Negative control (secondary antibody only). (G) Co-staining for pancytokeratin (green) and DAPI (blue, cell nuclei). (H) Timeline showing a rapid rise in the resistance of ruminal cells growing on filter supports (N=2). (I) Peak resistance value of cultures of ruminal (N=4) and omasal cells (N=5) 1 week after being reseeded from confluent primary cultures onto filter supports.

Typically, the first fractions obtained by this procedure only showed cellular detritus from the stratum corneum. Later fractions contained increasing numbers of small, round cells in a suspension that continued to contain large quantities of cellular material from the upper strata of the epithelium. Depending on the thickness of the overlying epithelium, the isolation of viable cells from the stratum basale of the omasum required a trypsinization time of 1.5 to 3.5 h. For rumen, trypsination frequently had to be extended to over 5 h. Subsequently, the epithelium was removed from the chamber and fixed in 4% formaldehyde solution for hematoxylin and eosin (H&E) staining.

After centrifugation, the entire cellular material of each fraction was resuspended in 4 ml M199 cell culture medium containing fetal calf serum (150 ml l^{-1}), L-glutamine (6.8 mmol l^{-1}), HEPES (20 mmol l^{-1}), nystatin (2.4×10^5 U l^{-1}), gentamycin (50 mg l^{-1}) and kanamycin (100 mg l^{-1}) (Biochrom AG or Sigma-Aldrich), and plated into cell culture dishes coated with collagen A (60 mm Ø, one for each fraction), all essentially as previously described (Galfi et al., 1993). The probability of establishing viable cultures was found to depend on the presence of the small, round cells preferentially found in later fractions. A density of greater than 100 cells cm^{-2} was desirable.

After 1 day in culture, non-attached cell detritus was carefully removed by repeated washing with Ca^{2+}-free PBS buffer solution. After 1.5 to 2 weeks, the cells were split at a ratio of 1:2 for further culture in DMEM medium (Pan Biotech GmbH, Eidenbach, Germany; with 4.5 g l^{-1} glucose, 3.7 g l^{-1} $NaHCO_3$ and L-glutamine) supplemented with fetal calf serum (10%), HEPES (2%) and penicillin/streptomycin (1%).

H&E staining and staining for cytokeratin and vimentin

Immediately after transport to the laboratory (intact tissue) or after removal from the incubation chamber (trypsinized tissue), tissue samples were fixed in formalin. After a maximum of 48 h (at 4°C), tissues were embedded in paraffin and cut at 3 µm. Tissue sections were stained with H&E for histological examination using routine procedures. For vimentin and cytokeratin staining, cells were washed three times in PBS buffer, fixed with 4% paraformaldehyde (PFA) for 15 min, washed, permeabilized with 0.1% Triton X, washed again, and blocked with a goat-serum-containing blocking buffer. Subsequently, cells were incubated for 1 h in a PBS buffer containing 2% bovine serum albumin without (controls) or with specific antibodies (at a dilution of 1:100) for staining. Controls and antibody-treated cells were incubated with a fluorescence-labelled secondary antibody (1:100 in PBS). Vimentin and cytokeratin antibodies (mouse, AE-1 and pancytokeratin) were obtained from Dako Cytomation (Glostrup, Denmark; Clone V9) and Invitrogen (Carlsbad, CA, USA), respectively. The FITC-conjugated anti-mouse secondary antibody was obtained from Sigma-Aldrich, and all other reagents were either from Carl Roth GmbH (Karlsruhe, Germany) or from Sigma-Aldrich.

Staining for tight junction proteins

Cultured cells were seeded onto filter supports (pore size 0.4 µm, 0.6 cm^2, Millicell-PCF, Millipore, Schwalbach, Germany) at a density of 10^5 cells cm^{-2} and grown to confluence. Subsequently, cells were washed with PBS and fixed with methanol (10 min, –20°C).

Tissue samples were fixed in 4% PFA for 3 h, followed by 5 min exposure to 25 mmol l^{-1} glycine in PBS and successive incubation in 10, 20 and 30% sucrose in PBS for at least 60 min each. Samples were then frozen in liquid-nitrogen-cooled methylbutane and mounted in a cryostat using Tissue-Tek® OCT compound (Sakura, Zoeterwoude, The Netherlands), cut into 10 µm sections and mounted on glass slides. Slides were boiled for 15 min in EDTA buffer (1 mmol l^{-1} EDTA, pH 8, adjusted with NaOH) to unmask antibody binding sites.

Fixed cells and cryosections were permeabilized with 0.5% Triton X-100 solution and blocked with 1 and 5% goat-serum in PBS, respectively. Staining was carried out using the following primary and secondary antibodies: m-anti-caveolin-1 (BD Biosciences Pharmingen, San Diego, CA, USA), rb-anti-claudin-1, -2, -3, -5, -7, -8 and -10, m-anti-claudin-4, rb- and m-anti-occludin (Invitrogen), Alexa Fluor 488 goat anti-mouse and Alexa Flour 594 goat anti-rabbit (Invitrogen) at dilutions of 1:100 for primary and 1:500 for secondary antibodies. Controls were stained with secondary antibodies only. Nuclei were stained using 4′,6-diamidino-2-phenylindole dihydrochloride (DAPI; final concentration 1 µmol l^{-1}). Images were obtained using a confocal laser microscope (Zeiss LSM510, Carl Zeiss, Jena, Germany) at 543, 488 and 405 nm.

RNA isolation

Total RNA was extracted from sheep rumen and omasum using the NucleoSpin® RNA/protein kit (Macherey-Nagel, Düren, Germany), according to the manufacturer's directions. During this routine, genomic DNA was digested to avoid artefacts. cDNA was synthesized from 4 µg total RNA using the High Capacity cDNA Archive Kit (Applied Biosystems, Foster City, CA, USA) in a 40 µl reaction volume.

For screening, PCRs were performed with HOTSTAR DNA polymerase (Qiagen, Hilden, Germany). All primers are listed in supplementary material Table S1. Cycling conditions were: 30 s 95°C, 30 s 58 or 61°C and 60 s 72°C for 35 cycles with an initial denaturation of 15 min and final extension of 10 min. PCRs yielding positive results were repeated using PfuTurbo® DNA polymerase (Stratagene, La Jolla, CA, USA). Cycling conditions were as described above except that the initial denaturation was shortened to 2 min. PCR products were ligated into pCR®2.1-TOPO (Invitrogen) and sequenced (ABI310 Sequencer, Applied Biosystems).

Protein extraction

Sheep rumen and omasum was homogenized in lysis buffer (20 mmol l^{-1} TRIS, 5 mmol l^{-1} $MgCl_2$, 1 mmol l^{-1} EDTA, 0.3 mmol l^{-1} EGTA) containing protease inhibitors (Complete, Boehringer, Mannheim, Germany). Membrane proteins were extracted and blotted as recently described in detail (Milatz et al., 2010). Proteins were detected using rb-anti-claudin-1, -2, -3, -5, -7 and -8, and m-anti-claudin-4 and m-anti-occludin antibodies (Invitrogen, dilutions 1:2000 for all except occludin and claudin-1 which were used at 1:1000), and visualized by luminescence imaging [Lumi-Light^{PLUS} Western Blotting Kit (mouse/rabbit), Roche Applied Science, Mannheim, Germany; LAS-1000, Fujifilm, Tokyo, Japan].

Transepithelial resistance measurements

For measurements of transepithelial resistance (TER), cultured cells were seeded onto filter supports (pore size 0.4 µm, 0.6 cm^2, Millicell-PCF, Millipore) at a density of approximately 10^5 cells cm^{-2}. TER was measured using 'chopstick' electrodes (STX-2, World Precision Instruments, Berlin, Germany) as previously described (Schmitz et al., 2002).

Patch-clamp experiments

For patch clamping, cultured cells were seeded onto glass coverslips at low density (approximately 2000 cells cm^{-2}). Experiments were usually performed on the following two days; confluent cells could not be used because of electrical coupling *via* gap junctions.

Pipettes were pulled with a DMZ-Universal puller (Zeitz-Instruments, Munich, Germany) using borosilicate glass capillaries (Harvard Apparatus, Holliston, MA, USA). Currents were recorded using an EPC 9 patch-clamp amplifier (HEKA Elektronic, Lambrecht, Germany) using commercially available software (TIDA for Windows, HEKA Elektronic). Positive ions flowing into the pipette correspond to a negative current and are depicted in the figures as going downwards.

Two types of pulse protocols were applied. Conventional voltage pulse protocols were used that recorded data at a sampling rate of 5 kHz. Voltage was increased from –120 to 100 mV for a duration of 50 ms in steps of 10 mV, returning to a holding potential of –40 mV between each step. Alternatively, current responses were recorded at 100 Hz by using a protocol that generated steps of 200 ms duration to voltages between –120 and 100 mV in 20 mV steps, returning to a holding potential of –40 mV for 200 ms between each step. This protocol was repeated continuously to allow the monitoring of current responses of the cells to changes in external solution.

The pipette solution for whole-cell experiments contained (in mmol l^{-1}) 138 Na^+, 128.2 gluconate, 1.1 Mg^{2+}, 2 Ca^{2+}, 5 K^+, 1 $H_2PO_4^-$, 20 Cl^-, 5 EGTA (corresponding to $[Ca^{2+}]_{free}$ ~10^{-7} mol l^{-1}) and 10 Hepes (7.2/Trizma). Extracellular solutions contained (in mmol l^{-1}) 138 Na^+, 128.2 of the anion as indicated and 0.9 Mg^{2+}, 1.7 Ca^{2+}, 5 K^+, 1 $H_2PO_4^-$, 19 Cl^- and 10 Hepes (7.4/Trizma). Osmolarity was adjusted to 290 mosmol l^{-1} with the dominant salt. Diisothiocyanato-stilbene-2,2′-disulfonic acid (DIDS) was dissolved in dimethyl sulfoxide (DMSO) to yield a stock solution that was stored at –20°C and protected from light throughout. The blocker was added to the experimental solutions at a ratio of 1:1000 immediately before experiments, with a final concentration of 200 μmol l^{-1}.

All perfusion solutions were warmed to 37°C immediately before infusion into the 200 μl perfusion chamber *via* a perfusion cannula (PH01, Multi Channel Systems, Reutlingen, Germany) connected to a temperature controller (TC01/2, Multi Channel systems). The solutions were applied *via* two separate but identical pumps (MS/CA4/840, Ismatec, Glattbrugg-Zürich, Switzerland), both of which were equipped with four parallel lanes of high-precision Tygon tubing (Ismatec) to ensure identical flow rates (4 ml min^{-1}). This setup has previously been described in more detail (Stumpff et al., 2009).

To compare whole-cell data from the different cells, currents were allowed to stabilize in NaCl solution for at least 3 min; cells that did not show stable current levels after this time were discarded. The current level at 100 mV pipette potential was then assigned a value of 100%. All other currents were expressed as a percentage of this value obtained at the beginning of the experiment.

Reversal potentials were estimated by linear regression between the current values at just above and just below the zero level for each cell and corrected for liquid junction potential according to established methods (Barry and Lynch, 1991). All values are given as means ± s.e.m and were tested for significance with the Mann–Whitney rank sum test (SigmaStat 3.0.1, IBM, Somers, NY, USA).

RESULTS

An improved method for the isolation of cells from forestomach epithelia

As described in more detail in the Materials and methods, forestomach tissue was clamped between the two sides of an Ussing-chamber-like device, allowing a selective exposure of the apical side of the tissue to a trypsin-containing buffer (see Fig. 1A). After the isolation procedure, the tissue could be removed and microscopically studied to identify the depth of the trypsin erosion (Fig. 1C). As expected, trypsinization had to proceed to the stratum basale of the tissue before viable cell cultures could be obtained.

Transepithelial resistance

Primary cultures were grown to confluence and reseeded at the same density onto permeable filter supports. TER was measured daily after reseeding and reached a plateau value after approximately 5 to 7 days. Mean plateau values for five cell preparations derived from the omasum and four preparations derived from the rumen were 1522±126 and 729±134 Ω cm^2, respectively (Fig. 1H,I).

Staining for cytokeratin, vimentin and occludin

Cultivated cells were characterized by immunostaining for cytokeratin, vimentin and occludin. Both the intact tissue and cells cultured from omasal and ruminal isolates could be shown to express cytokeratin using either an AE-1 or a pancytokeratin stain, with staining intensity of individual cells quite variable and highest in clusters of cells. At the edges of these islets, cells showed only weak staining for cytokeratin (Figs 1, 2).

Although cytokeratin staining suggests an epithelial origin of the cells, the cells also showed staining for vimentin, which is frequently used to stain fibroblasts (Fig. 2E,G). For this reason, co-staining for occludin was carried out. Occludin is a tight junction protein that is characteristically expressed by the barrier-forming cells of epithelia and endothelia, but not by cells originating from connective tissues such as fibroblasts.

Confluent cells in culture showed occludin staining along all cellular junctions (Figs 3–6). Native tissue showed staining for occludin in all layers of the epithelium from the stratum granulosum down to the stratum basale (Figs 4–6). Cells of the stratum corneum and subepithelial cells did not react to occludin antibodies, apart from some staining along the endothelia of subepithelial capillaries (Fig. 5E). In multi-layered preparations, occludin staining was found in the apical-most cell layer facing the culture medium (Fig. 2F). However, staining for occludin could also be detected in deeper cell layers, where it was frequently localized within the cytosol and may reflect occludin not yet trafficked to the cellular membrane. Cells with staining for occludin mostly, but not always, also showed staining for cytokeratin, with maximal staining intensity around the cellular nuclei and below the occludin ring (Fig. 2C).

In multilayered preparations, cytokeratin staining was highest in the apical-most cell layers, whereas staining for vimentin could mainly be detected close to the filter support onto which the cells had been seeded (Fig. 2B,C,F,G). This initially appeared suggestive of a co-culture of fibroblasts and keratinocytes. However, upon closer inspection, numerous individual cells were found to clearly show co-staining for both vimentin and occludin (Fig. 2E,G).

Control experiments using the established epithelial cell line MDCK-C7 demonstrated co-expression not only of cytokeratin and occludin, but also of vimentin (Fig. 2H,I). Our findings confirm numerous previous studies reporting that epithelial cells – in particular when grown in culture – can express vimentin when in a state of proliferation (Ben-Ze'ev, 1984).

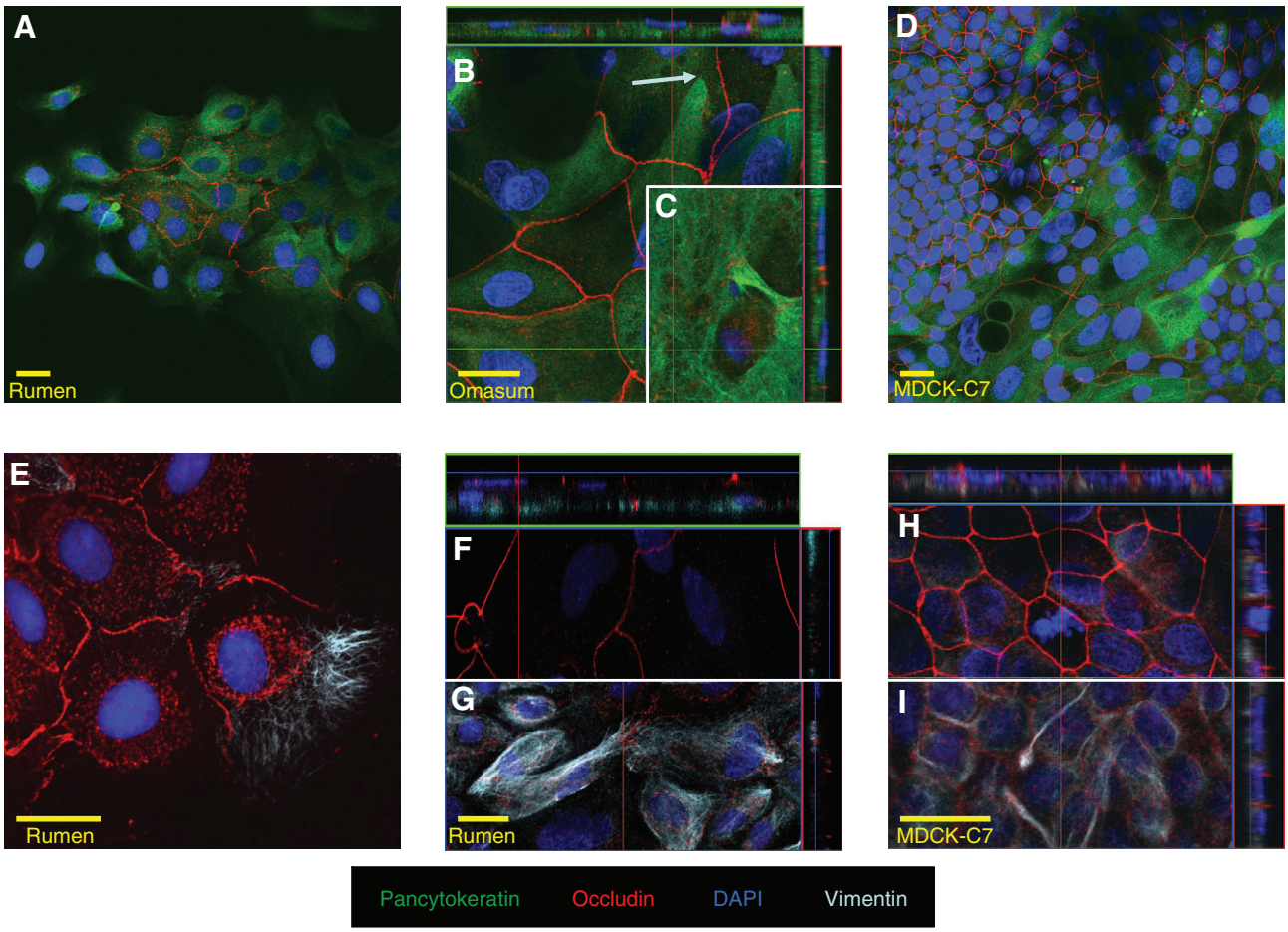

Fig. 2. Staining of cultured sheep cells for occludin (red), pancytokeratin (green), vimentin (light blue) and DAPI (dark blue, cellular nuclei). (A) Islet of subconfluent ruminal epithelial cells costained for pancytokeratin and occludin. Only cells at the center of the islet express occludin in the cellular junction, although cytosolic specks of red are visible in surrounding cells. (B,C) Confluent culture of omasal epithelial cells showing costaining for pancytokeratin and occludin. Z-stacks through preparations reveal a multilayered structure (apical side up, with *xz* and *yz* sections shown above and to the right of the large central image (*xy*), which represents the cells as seen when looking from above into the cell culture dish along the vertical *z*-axis). (B) An optical section through the apical layer of the preparation; (C) an optical section 3.43 μm further down towards the filter support. Sometimes, cells overlap so that cytokeratin appears to cross the cellular junction (light blue arrow). (D) Cells from the established epithelial cell line MDCK-C7, showing co-staining for cytokeratin and occludin. (E) Isolated islet of ruminal epithelial cells. A tuft of vimentin staining can be seen within a cell that also shows occludin staining. (F,G) Cells cultured from the ruminal epithelium, showing junctional staining for occludin apically (F), while staining for vimentin appears near the filter support 6.44 μm further down (G). (H,I) Monolayer of epithelial MDCK–C7 cells showing costaining for occludin and vimentin (H: apical, I: 3 μm further down). Scale bars, 20 μm.

Expression of claudins by native tissues and cultured cells

To gain a further insight into the barrier properties of the omasal epithelium, expression and localization of various claudins was investigated in western blots and immunostainings. As specificity of most claudin antibodies has not yet been established for sheep, verification was attempted by PCR.

Western blot

Western blots on protein extracts from omasal and ruminal tissue showed clear expression of occludin and claudins 1, 3 and 4. No specific staining was obtained for claudins 2, 5 and 8. Results for claudin-7 varied between different preparations. Protein extracted from the canine kidney cell line MDCK-C7 or from the human colonic cell line HT-29/B6 served as control (Fig. 7).

PCR

PCR was carried out on cDNA prepared from sheep omasal tissue. As full sequences for sheep claudin mRNA are not yet known, primers were designed using the non-coding regions of bovine mRNAs. All primers are listed in supplementary material Table S1. Using this strategy, the coding sequences of three claudin mRNAs could be identified and fully sequenced, namely claudin-1, -4 and -7 (GenBank accession numbers HM117762, HM117763 and HM142819, respectively; see supplementary material Table S2). Compared with cattle, mRNA coding sequences (CDSs) showed 99% (claudin-1 and -7) and 98% (claudin-4) identity, respectively. This results in the exchange of two, four and three amino acids for claudin-1, -4 and -7, respectively. Compared with human sequences, these values were 91% (claudin-1 and -7) and 88% (claudin-4) mRNA CDS identity, resulting in 17, 26 and 16 amino acid exchanges for claudin-1, -4 and -7, respectively.

Immunostaining for claudins

Claudin-1, -4 and -7

In keeping with the above findings, staining for claudins 1, 4 and 7 and for occludin could be found both in native tissue and in cultured cells of sheep rumen and omasum (Figs 3, 4).

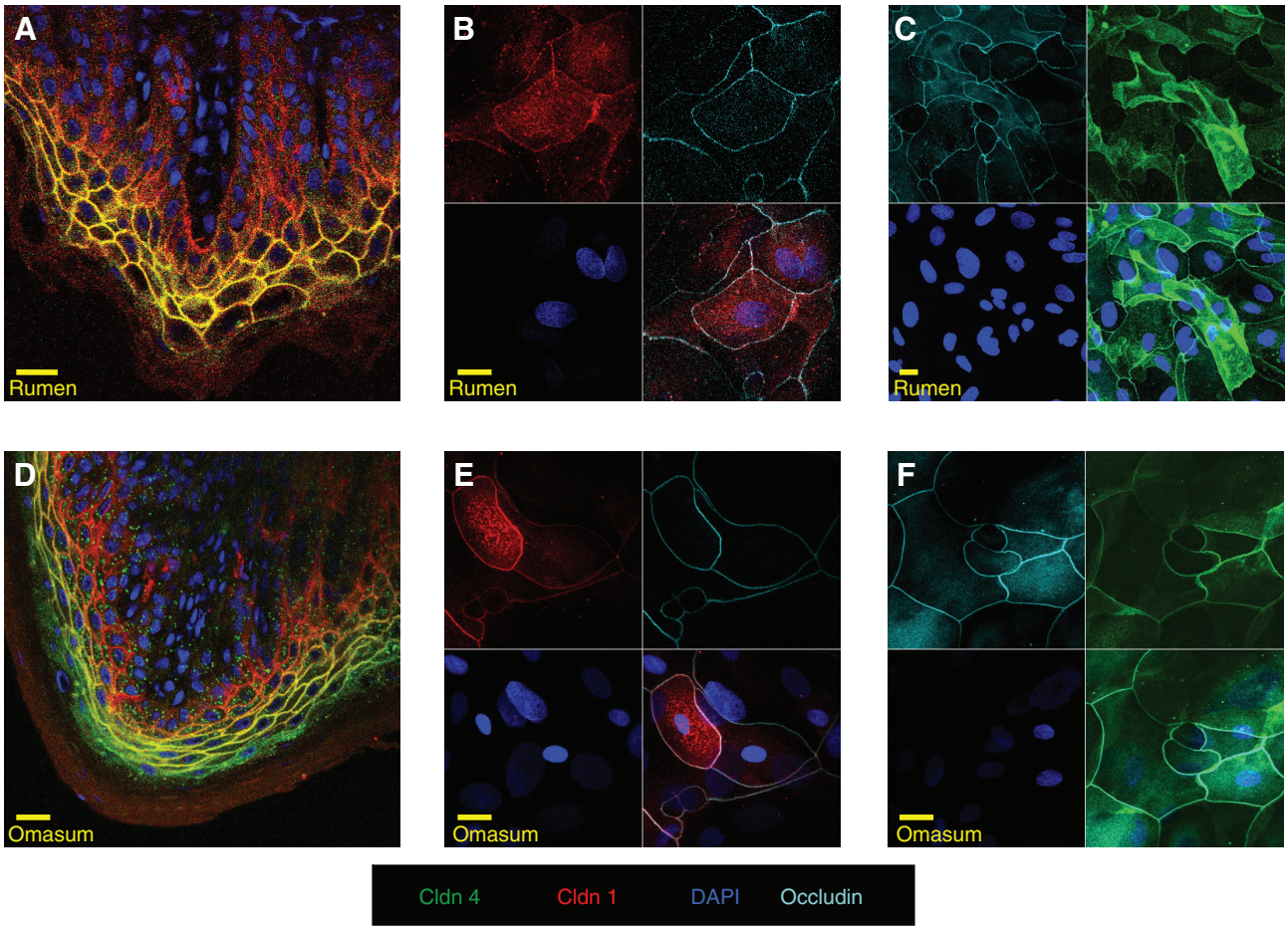

Fig. 3. Staining for claudin-1 (red), claudin-4 (green), occludin (light blue) and DAPI (dark blue) in the omasum and rumen of sheep. (A) Native epithelium of the rumen, co-stained for claudins 1 and 4. Colocalization of claudin-1 and claudin-4 within the apical layer results in yellow. (B) Detail from a culture of ruminal epithelial cells, co-stained for claudin-1 (upper left), occludin (upper right), and DAPI (lower left) with an overlay of all three stainings shown in the lower right panel. Note that the four panels all show the same cells, but that each panel highlights staining for a different protein. (C) Cultured ruminal cells, co-stained for occludin (upper left), claudin-4 (upper right) and DAPI (lower left). As in B, all four panels of the figure again show the same detail, with an overlay of all stainings in the lower right panel. (D) Native omasal epithelium, costained for claudins 1 and 4. (E,F) Cultured cells of the omasum, stained as in B and C. Scale bars, 20 μm.

In tissue sections, staining for claudin-1 reached the stratum basale and showed a slight tendency to decrease apically towards the stratum granulosum, whereas staining for claudin-4 was inversely distributed, with the most intensive staining found in the apical layers. Costaining for both claudins was apparent in large parts of the epithelium of both the rumen and the omasum. The stratum corneum did not stain for either occludin, claudin-1 or claudin-4. Conversely, claudin-7 staining was found almost exclusively in cells of the stratum corneum, and did not colocalize with occludin.

Cultured cells showed robust staining for claudins 1 and 4, which were found to colocalize with each other along the cellular boundaries as seen in the native epithelia. In contrast to the native tissue, occludin and claudin-7 were found to colocalize with each other in the cell cultures. No differences could be detected between cells of ruminal and omasal origin.

Claudin-2, -5, -8 and -10

No specific staining was observed for claudins 2, 5, 8 (Fig. 5) and 10 (data not shown). Staining for claudin-2 and claudin-8 was found in the cytosolic space of both cultured and native epithelial cells from the rumen and the omasum, suggesting a nonspecific interaction with cytosolic proteins. No staining was observed in the subepithelial space. Because no colocalization with occludin was observed and the proteins were not detected in western blots, an unspecific reaction appears likely.

Antibodies against claudin-5 did not specifically stain the intact epithelium. Conversely, strong staining could be observed along the endothelia of the subepithelial capillaries (Fig. 5E). Cells in culture sometimes showed a diffusive staining of the cytosolic space for claudin-5, but a membrane-bound staining pattern suggesting specificity was not observed.

Staining for clauding-10 was detected neither in tissue nor in cultured cells.

Claudin-3

In the intact tissues of the rumen and the omasum, antibodies against claudin-3 stained the epithelial cell layers in a diffuse manner limited to the cytosolic space (Fig. 6A,C,E). No staining of subepithelial tissues was observed. In the cultures, most cells showed either no interaction with claudin-3 antibodies or only a diffuse and presumably nonspecific staining of the cytosol. However, a few cells

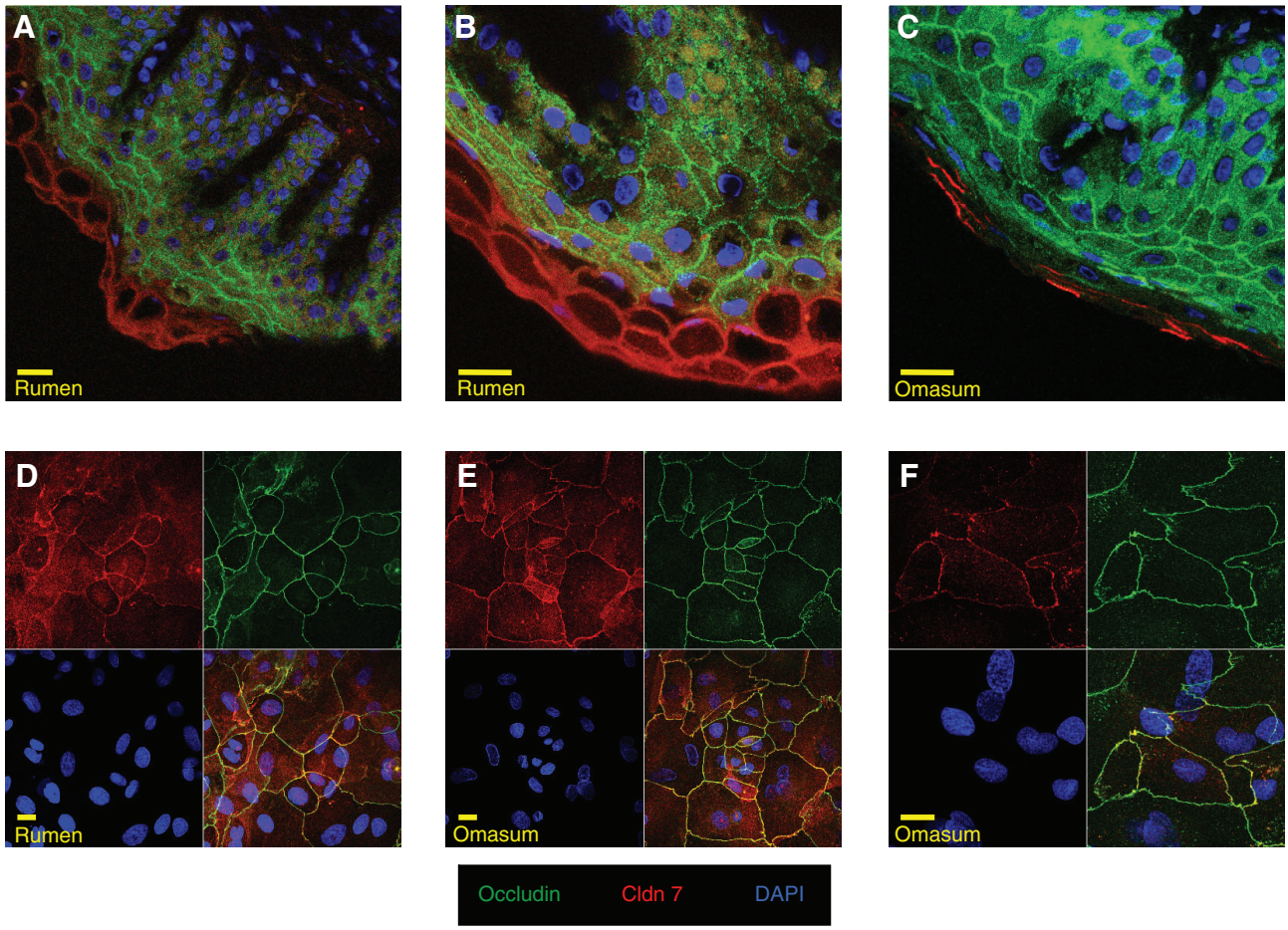

Fig. 4. Staining for claudin-7 (red), occludin (green) and DAPI (dark blue) in the omasum and rumen of sheep. (A,B) Native ruminal tissue. Occludin staining can be seen from the stratum basale to the stratum granulosum, whereas the claudin-7 signal is only detected in the nuclei-free top cell layers that appear to correspond to the stratum corneum. (C) Native omasal tissue, showing a similar staining pattern. (D–F) Cultured ruminal (D) and omasal (E,F) cells, showing coexpression of claudin-7 (upper left panels) and occludin (upper right panels) colocalized at cell boundaries (yellow, lower right panels). An overlay of all stainings is shown in the lower right panels. Scale bars, 20 μm.

showed staining for claudin-3 that clearly colocalized with occludin; the surrounding cells did not show staining (Fig. 6B,D,F).

Because claudin-3 is known to be expressed by cells of endothelial origin, a contamination of the cultures with endothelial cells from the capillaries under the epithelium was considered. However, staining for caveolin-1, which is expressed by cells of endothelial origin (Frank et al., 2007), was cytosolic and presumably unspecific (Fig. 6E,F), although specks of caveolin-1 staining were detectable along the capillaries of the intact epithelium. In conjunction, these results do not support a subepithelial origin of the cells expressing claudin-3.

Patch-clamp experiments

We have previously reported that ruminal epithelial cells express an anion channel permeable not only to chloride, but also to acetate (Stumpff et al., 2009). A conductance with the same properties could be observed in ruminal epithelial cells obtained with the new isolation method (N=5, data not shown).

A similar conductance could also be observed in omasal cells (Fig. 8). Currents of cells filled with a Na–gluconate solution and superfused with an NaCl buffer were outwardly rectifying, with reversal potential at –30±2 mV (N=41). Because all ions except chloride and Ca^{2+} (out>>in) were in equilibrium across the membrane, this negative reversal potential must reflect the influx of chloride into the cell.

Correspondingly, the current at +100 mV pipette potential was reduced to 34±3% of the initial value when chloride was replaced by gluconate in the external solution (P<0.001, N=41). When acetate was the dominant anion in the bath solution, current at +100 mV was significantly higher than that measured in Na–gluconate solution, but only 80±12% (N=28) of the value measured in NaCl solution (P<0.001).

Reversal potential rose significantly with the size of the anion in the bath solution, from –30±2 mV (N=41) in NaCl solution to –6±7 mV (N=28) in the Na–acetate solution to +10±2 mV in the Na–gluconate solution (all P<0.001). Because the cells were filled with a Na–gluconate solution so that Na^+ and K^+ were in equilibrium across the membrane, the changes in reversal potential could not have been caused by a stimulation of cationic currents.

This conclusion was supported by the effects of the anion channel blocker DIDS. DIDS (200 μmol l^{-1}) reduced current at +100 mV in NaCl solution to 57±6% of the initial value (P<0.001, N=23). In the Na–acetate solution, DIDS also had significant effects, with the current at +100 mV dropping from 79±9% of the value measured in the NaCl solution to 35±6% (P<0.001, N=25). Recovery after washout was complete (beginning NaCl *versus* end NaCl, P=0.9).

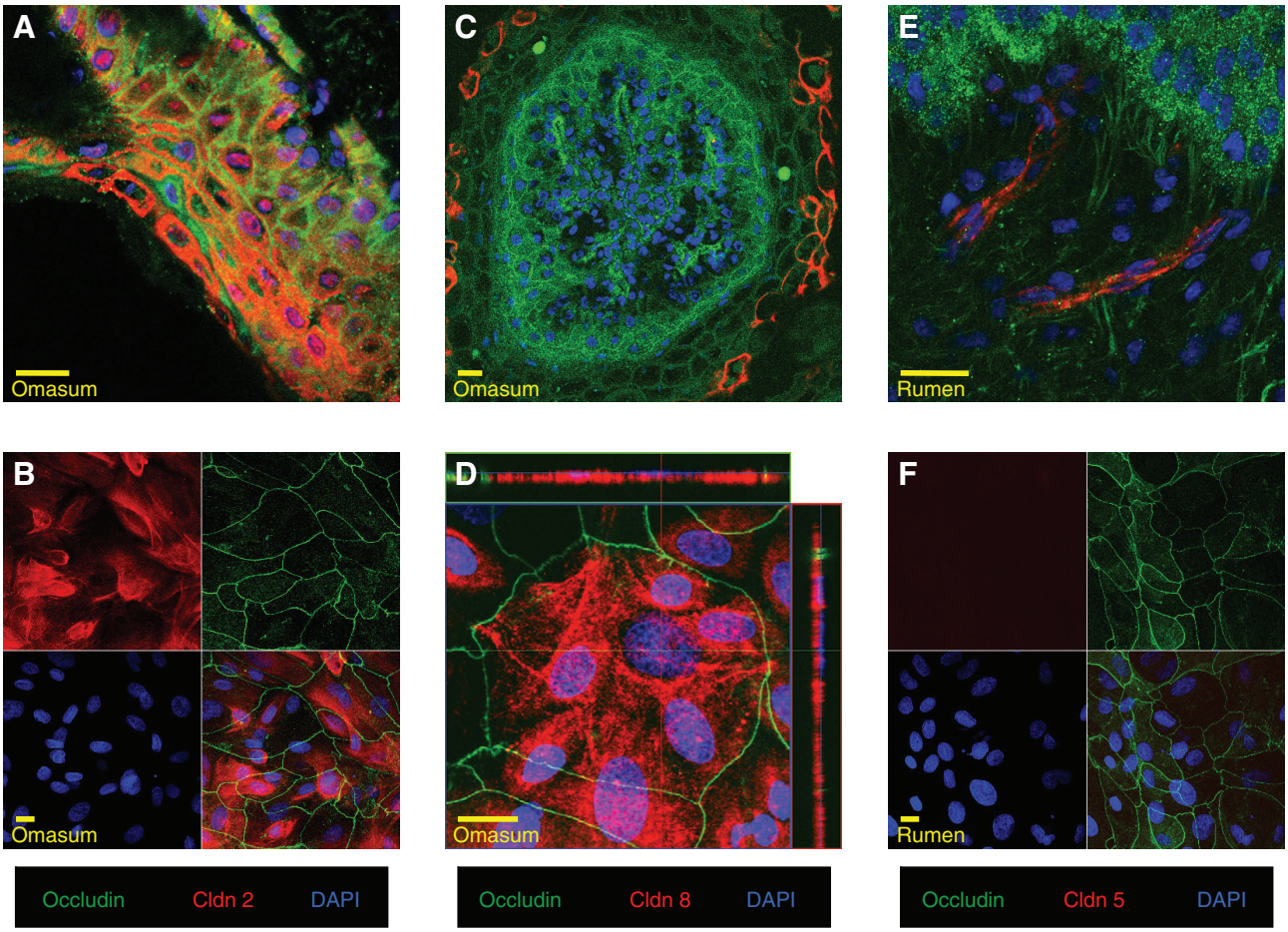

Fig. 5. Staining for claudin-2, -8 or -5 (red), occludin (green) and DAPI (dark blue) in the omasum and rumen of sheep. (A,B) Native forestomach epithelia and cultured cells show cytosolic staining for claudin-2 (B, upper left panel) that is most likely non-specific and does not colocalize with occludin (B, upper and lower right panels). Subepithelial cells do not show any staining. (C,D) A similar staining pattern can be observed for claudin-8. D is a multi-stack image (compare Fig. 2), with *xz* and *yz* sections shown above and to the right of the central image (*xy*). The preparation shown in D is probably multilayered, with one flat cell (dark blue nucleus, surrounded by large occludin ring) overlaying a number of smaller cells near the filter. Again, staining for claudin-2 is clearly cytosolic. (E) native forestomach epithelia do not express claudin-5. However, staining is visible along the subepithelial capillaries, probably reflecting expression of claudin-5 by endothelial cells. (F) Likewise, cultured cells from forestomach epithelia show no staining for claudin-5 (upper left panel), although occludin is expressed (upper right). An overlay of all stainings is shown in the lower right panels of B and F. Scale bars, 20 μm.

In summary, the results suggest that ruminal and omasal cells express a conductance with a permeability sequence of gluconate< acetate<chloride.

DISCUSSION

In the present study, we introduce a new method for the isolation and cultivation of epithelial cells from the rumen and the omasum.

Upon reaching confluence, cultured cells developed high values of TER, indicating the expression of functional tight junction proteins. This expression was further investigated using PCR, western blot and immunohistochemical techniques, demonstrating expression of occludin and claudins 1, 4 and 7 by native ruminal and omasal epithelia of the sheep and by cell cultures derived from these preparations. The coding sequences of these three sheep claudin mRNAs could be identified and fully sequenced for the first time. The data do not support a functional expression of claudins 2, 5, 8 and 10.

In whole-cell patch-clamp investigations, these cultured omasal cells express a conductance for acetate that may mediate basolateral efflux of SCFA anions, as previously reported for cells of the rumen (Stumpff et al., 2009).

A new method for the isolation and cultivation of cells from forestomach epithelia with development of barrier function

The method presented here allows a selective exposure of the apical membrane to trypsin buffer, thus minimizing the danger of a contamination of the cultures by cells detached from subepithelial layers. In contrast to the classic technique (Galfi et al., 1993), no time-consuming dissection of ruminal papillae is necessary. In addition, it is now also possible to isolate cells from tissues with short papillae, such as the omasum, which was not previously possible.

High TER values of >500 Ω cm^2 developed when the cells were grown on filter supports (Fig. 1H,I), corresponding to the expression of the sealing tight junction proteins claudin-1, -4 and -7, all of which could also be detected in the intact epithelia (Figs 3, 4). The TER values of the cells in culture exceeded those found in the intact epithelia, which are in the order of 300–500 Ω cm^2 [corresponding to conductances of 2–3 mS cm^{-2} (Abdoun et al., 2010)]. The

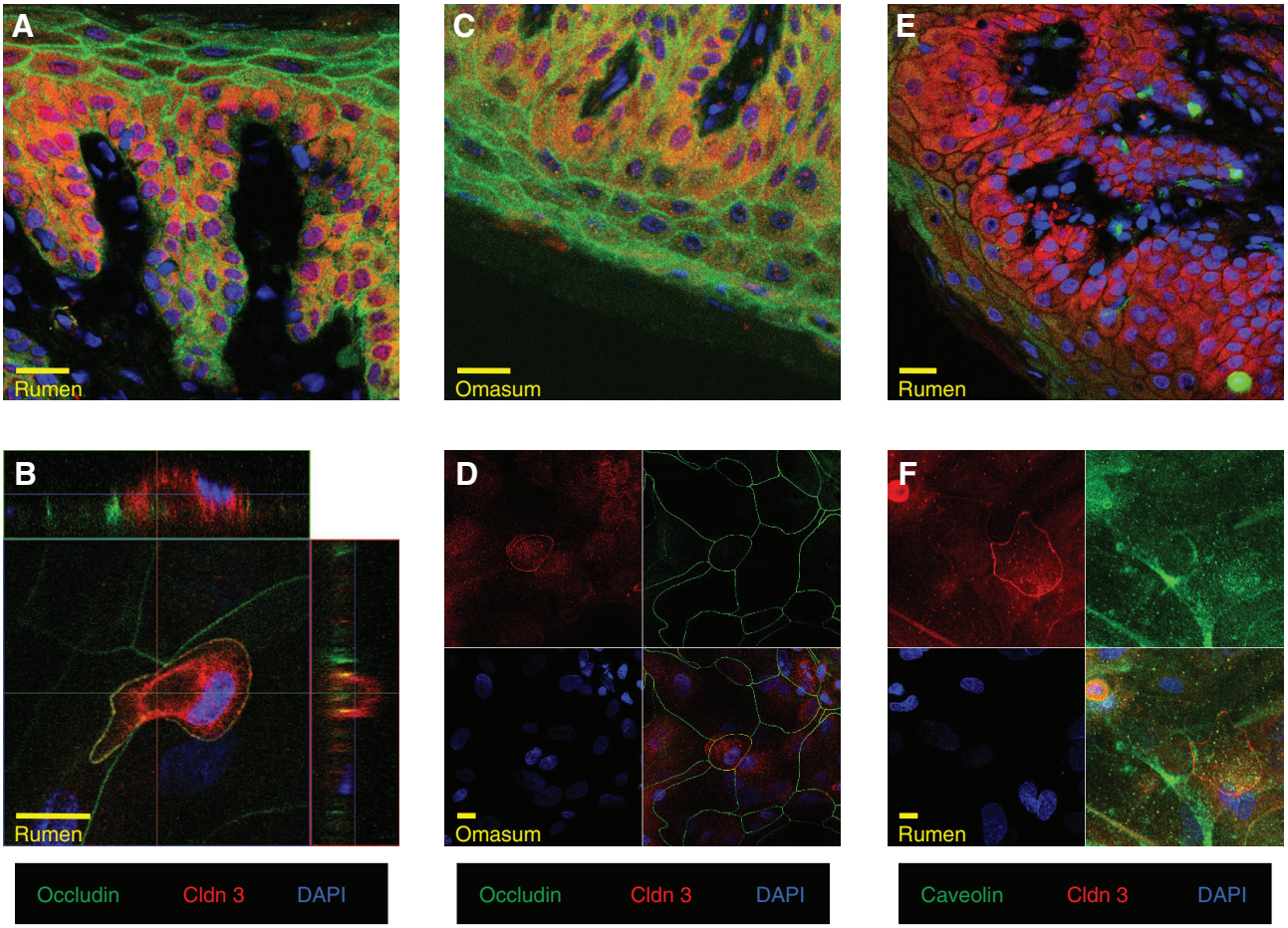

Fig. 6. Staining for claudin-3 (red), occludin or caveolin (green) and DAPI (dark blue) in the omasum and rumen of sheep. (A,B) Native tissue and cultured cells of the rumen, showing cytosolic staining for claudin-3 (red) and junctional staining for occludin (green). B is a three-dimensional multi-stack image, with *xz* and *yz* sections shown above and to the right of the central image (*xy*). (C,D) Native tissue and cultured cells of the omasum, stained for claudin-3 (D, upper left panel) and occludin (D, upper right panel). (E,F) native tissue and cultured cells of the rumen, showing diffuse cytosolic staining for claudin-3 (F, upper left panel) and caveolin (F, upper right panel). Specks of caveolin can be seen in the subepithelial space that may reflect staining of endothelial cells. In the cultured cells (B,D,F), a few isolated cells can be seen to express claudin-3 along the cellular junction, clearly co-localized with occludin (yellow staining in the overlay). An overlay of all stainings is shown in the lower right panels of D and F. Scale bars, 20 μm.

somewhat higher values of cultured cells can readily be explained by the fact that the surface area of the intact epithelium is amplified by numerous papillae.

Cells tended to grow larger and flatter with every week in culture. For this reason, older cultures were not utilized for experiments in the past (Stumpff et al., 2009). The present study revealed that when in a confluent layer, such large cells show a robust expression of occludin (Fig. 2F) and morphologically resemble the larger and flatter cells of the stratum granulosum (Fig. 3), suggesting maturation rather than dedifferentiation. Underneath these larger cells, smaller cells could be observed that showed staining for vimentin (Fig. 2G).

An initial working hypothesis that this reflected a co-culture of fibroblasts and keratinocytes was eventually rejected. First, subconfluent cultures in which all cells showed vimentin staining also stained for cytokeratin, suggesting a coexpression of both proteins by the same cells. Second, we were able to clearly demonstrate co-expression of occludin and vimentin by individual ruminal and omasal epithelial cells (Fig. 2E–G). Because fibroblasts do not form intercellular junctions (Shen et al., 2010), these cells cannot be fibroblasts. Vimentin and tight junction proteins were also co-expressed in the established epithelial cell line MDCK-C7. We therefore confirm the results of previous studies (Ben-Ze'ev, 1984; van der Velden et al., 1999), suggesting that vimentin is not a suitable marker for fibroblast contamination. In summary, no conclusive evidence supporting a co-culture with cells of non-epithelial origin could be found.

Forestomach epithelia express claudins 1, 4 and 7

The classic model according to which the barrier function of the rumen is maintained by a single layer of cells within the stratum corneum persists unto the present day (Cunningham, 2002), but has been refuted by numerous studies demonstrating the expression of 'occluding junctions' by cells from the stratum granulosum (Schnorr and Wille, 1972) to the stratum basale of both the rumen and the omasum (Scott et al., 1972). These older findings are confirmed by the only recent study demonstrating an expression of claudin-1 and ZO-1 by all cell layers except for the stratum corneum (Graham and Simmons, 2005). In the same study, the density of mitochondria and the expression of the Na^+/K^+-ATPase was found to be clearly

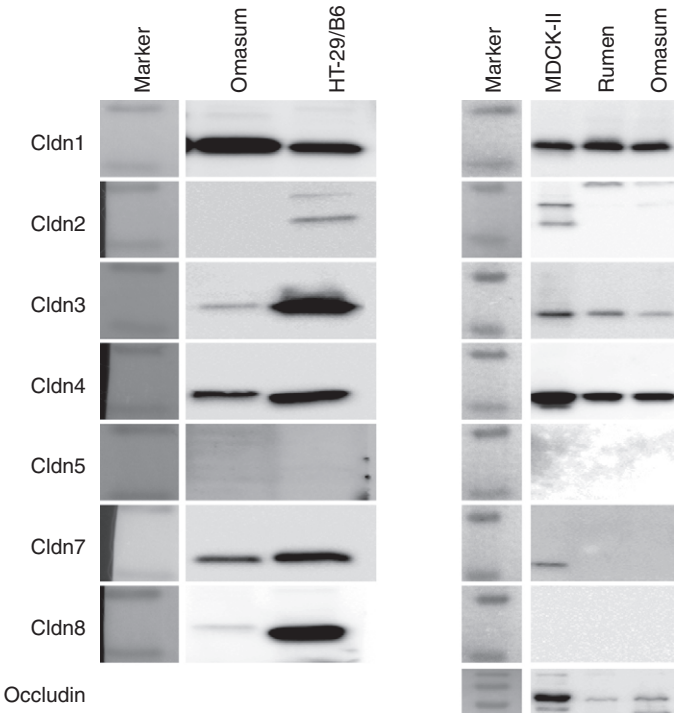

Fig. 7. Claudin expression (western blot). Expression of claudins 1 and 4 can be seen in protein extracts from both omasal and ruminal sheep tissue. No specific staining was obtained for claudins 2, 5, and 8, staining for claudin-3 was weak (see Discussion). Results for claudin-7 varied between different preparations. Protein extracts from the canine kidney cell line MDCK-II or from the human colonic cell line HT-29/B6 served as control.

highest toward the basal plasma membrane of the stratum basale, while cells of all layers were connected by gap junctions (connexins 43 and 26). The ruminal epithelium thus represents a functional syncitium of tightly interconnected cells.

In our hands, staining for claudin-1 resembled that found by Graham and Simmons (Graham and Simmons, 2005), although we observed a more intense staining of the cellular junctions in basal epithelial layers. Claudin-4 staining was almost exclusively found within the stratum granulosum and spinosum. Claudin-7 appeared in low density in the bottom layers of the stratum corneum, possibly corresponding to the 'occluding junctions' previously found within this layer of cells (Henrikson and Stacy, 1971; Schnorr and Wille, 1972), but did not stain the rest of the epithelium. Data on claudin-3 remain contradictory, possibly because of a lack in specificity of the claudin-3 antibody in sheep tissue. In all, our data on claudin-1, -4 and -7 expression are consistent with findings in skin (Kirschner et al., 2010) and esophagal epithelium (Lioni et al., 2007).

The barrier function of forestomach epithelia

The paracellular pathway of forestomach epithelia appears to be remarkably impermeant to anions. Thus, chloride entering the rumen with saliva (10–40 mmol l^{-1}) under *in vivo* conditions is absorbed into blood against a considerable electrochemical gradient (Sperber and Hyden, 1952; Dobson and Phillipson, 1958; Martens et al., 1991), requiring that the paracellular pathway effectively prevents a reflux.

TERs can be expressed in equivalent electrical circuits as a transcellular resistance (R_c) and paracellular resistance (R_p) in parallel and a subepithelial resistance (R_s) in series to these two resistances. TER thus can be expressed by the following equation:

$$\mathrm{TER} = R_s + \frac{R_p \cdot R_c}{R_p + R_c} \quad . \qquad (1)$$

The R_s of cell layers grown on filter supports amounts to approximately 10 Ω cm^2 (Krug et al., 2009). As can be deduced from Eqn 1, neither R_c nor R_p can be smaller than TER–R_s.

The present study thus suggests that R_p is larger than approximately 720 Ω cm^2 (rumen) and 1510 Ω cm^2 (omasum) and that claudins 1 and 4 are involved in maintaining this barrier, in line with the sealing properties attributed to these claudins (Van Itallie and Anderson, 2006; Shen et al., 2010). Because the expression pattern of claudin 7 by the basal parts of the stratum corneum was discontinuous, a major role of this tight junction protein in functional epithelial barrier formation in the tissues studied appears unlikely.

Impact of present findings on models for ruminal and omasal SCFA absorption

It has long been known that acetate and propionate serve as a major source of energy for the ruminant and are thus absorbed unmetabolized into the portal blood (Phillipson and McAnnally, 1942; Kristensen, 2005). Because a major fraction of the protons produced in the fermentational process are removed *via* salivary buffering (Allen, 1997; Aschenbach et al., 2010), the anions of SCFA do not leave the rumen coupled to an equimolar amount of protons. The argument is even more pressing for the omasum, as only small quantities of SCFA are produced locally and the digesta enter the omasum from the rumen in a well-buffered state. The proton concentration is thus negligible and SCFA have to be absorbed from the omasum in a net process that involves the co-transport of strong cations, which requires transport mechanisms other than diffusion of lipophilic non-dissociated SCFA directly through the lipid bilayer (lipid diffusion).

For this reason, an early study suggested that significant amounts of SCFA anions might be absorbed from the rumen through paracellular 'water-filled pores', accompanied by a roughly equivalent amount of sodium (Danielli et al., 1945). However, this hypothesis contradicts multiple lines of evidence suggesting that forestomach epithelia form a tight barrier against the uncontrolled paracellular efflux of substrate. Thus, it was found that application of a transepithelial potential did not significantly affect the transport of SCFA (Stevens and Stettler, 1966). In addition, a paracellular pathway permeable to anions would lead to a large influx of chloride from plasma into the rumen, which cannot be observed *in vivo*. However, the conundrum initially raised by Danielli (Danielli et al., 1945) has not yet been satisfactorily resolved.

The expression of tight junction proteins sealing the paracellular pathway of the rumen and the omasum, together with the presence of a membrane channel for organic anions, supports the hypothesis that absorption of SCFA occurs *via* a transcellular pathway. Whereas apical uptake of butyrate is thought to primarily involve lipid diffusion with subsequent metabolization, numerous arguments suggest that transport of acetate may at least partially follow the outlines of NaCl transport across absorbing epithelia. In these tissues, the uptake of Na^+ *via* apical Na^+/H^+ exchange (NHE) and basolateral Na^+/K^+-ATPase is functionally coupled to the uptake of Cl^- *via* an apical anion exchanger and a basolateral anion channel, the latter being essential for providing the necessary charge balance for basolateral Na^+ export (Bachmann et al., 2011).

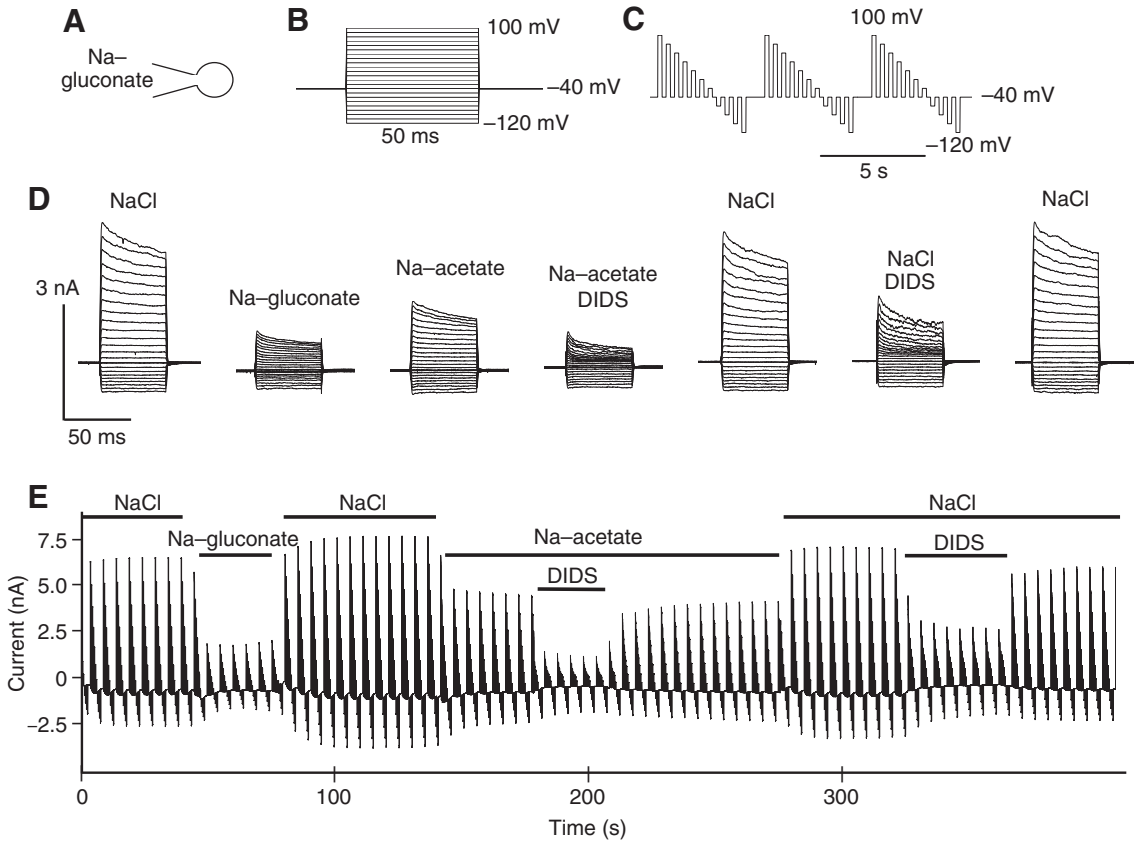

Fig. 8. Conductance of sheep omasal cells to chloride and acetate. Original recordings obtained from cultured omasal cells, showing the current response in different solutions. Cells were studied in the whole-cell configuration using a Na–gluconate pipette solution (A) and different pulse protocols (B, protocol I; C, protocol II; see Materials and methods). (D) The current response of one omasal cell to the pulse protocol shown in B. (E) The response of another cell exposed to the continuous pulse protocol shown in C. It can be seen that the current at +100 mV varies with the anions in the bath, reflecting an influx into the cells *via* a DIDS-sensitive pathway.

Anion transporting proteins are generally poorly selective, and both the apical anion exchanger (Aschenbach et al., 2009) and the basolateral anion channel (Stumpff et al., 2009) of the ruminal epithelium have recently been shown to accept acetate as a substrate. The present study suggests that omasal cells express a similar channel. Seen in conjunction, the sealing of the paracellular pathway and the presence of this anion channel represent the first unequivocal finding of protein-mediated transport of SCFA by cells of the omasal epithelium. We propose that basolateral efflux of acetate occurs through this channel, facilitated by the potential generated by the Na^+/K^+-ATPase. The parallel uptake of sodium and acetate by forestomach epithelia can thus be explained without having to challenge the barrier-forming properties of these tissues.

This model has important implications for tissue homeostasis. Because acetate enters the epithelium either directly coupled to a proton [*via* what is probably lipid diffusion (Ali et al., 2006)] or in exchange for buffering HCO_3^- (Aschenbach et al., 2009), but leaves the tissue without a proton, the amount of acetate that can be transported without damage is limited by the capacity of pH regulatory mechanisms. Accordingly, breakdown of barrier function is frequently observed in situations with high ruminal SCFA concentrations and low pH (Plaizier et al., 2008). More research is necessary to determine whether the breakdown of ruminal barrier function that occurs in these situations involves cellular necrosis, changes in the tightness of paracellular junctions, or both.

Barrier function aligns with expression of tight junction proteins by the rumen and the omasum

In summary, a new method is presented that allows the isolation of cells from the rumen and the omasum. In culture, these cells differentiate to express cytokeratin, occludin and claudins 1, 4 and 7 and are thus of epithelial origin; when grown to confluence, functional barrier formation can be demonstrated *via* TER measurements. We present evidence for the expression of the same library of tight junction proteins by the native epithelia of the rumen and the omasum, with expression of claudin-1 reaching down to the stratum basale. Finally, we demonstrate that, as previously shown for the rumen, omasal cells express an anion conductance permeable to chloride and acetate, thus enhancing the argument for a protein-mediated, transcellular uptake pathway for SCFA and arguing against paracellular efflux. We conclude that epithelial cells of the rumen and the omasum have extensive barrier-forming properties, aligned with the expression of tight junction proteins.

LIST OF ABBREVIATIONS

Cldn	claudin
DAPI	4′,6-diamidino-2-phenylindole dihydrochloride
DIDS	4,4′-diisothiocyano-2,2′-stilbenedisulfonic acid
EDTA	ethylenediaminetetraacetic acid
EGTA	ethylene glycol tetraacetic acid
H&E	hematoxylin & eosin
HEPES	4-(2-hydroxyethyl)-1-piperazineethanesulfonic acid
PBS	phosphate buffered saline

SCFA	short-chain fatty acid
TER	transepithelial resistance
VFA	volatile fatty acid (=SCFA)

ACKNOWLEDGEMENTS

We thank Jana Enders for expert help with H&E staining and Gabriele Kiselowsky for help with the cell cultures. The financial support of the Deutsche Forschungsgemeinschaft (DFG STU 258/4-1 and DFG Research Unit FOR 721/2), the Margarete Marcus Charity, and the Schaumann Stiftung is gratefully acknowledged.

REFERENCES

Abdoun, K., Stumpff, F., Rabbani, I. and Martens, H. (2010). Modulation of urea transport across sheep rumen epithelium *in vitro* by SCFA and CO_2. *Am. J. Physiol.* **298**, G190-G202.

Ali, O., Shen, Z., Tietjen, U. and Martens, H. (2006). Transport of acetate and sodium in sheep omasum: mutual, but asymmetric interactions. *J. Comp. Physiol. B* **176**, 477-487.

Allen, M. S. (1997). Relationship between fermentation acid production in the rumen and the requirement for physically effective fiber. *J. Dairy Sci.* **80**, 1447-1462.

Aschenbach, J. R., Bilk, S., Tadesse, G., Stumpff, F. and Gäbel, G. (2009). Bicarbonate-dependent and bicarbonate-independent mechanisms contribute to nondiffusive uptake of acetate in the ruminal epithelium of sheep. *Am. J. Physiol.* **296**, 1098-1107.

Aschenbach, J. R., Penner, G. B., Stumpff, F. and Gabel, G. (2010). Role of fermentation acid absorption in the regulation of ruminal pH. *J. Anim. Sci.* **89**, 1092-1107.

Bachmann, O., Juric, M., Seidler, U., Manns, M. P. and Yu, H. (2011). Basolateral ion transporters involved in colonic epithelial electrolyte absorption, anion secretion and cellular homeostasis. *Acta Physiol.* **201**, 33-46.

Barry, P. H. and Lynch, J. W. (1991). Liquid junction potentials and small cell effects in patch-clamp analysis. *J. Membr. Biol.* **121**, 101-117.

Ben-Ze'ev, A. (1984). Differential control of cytokeratins and vimentin synthesis by cell-cell contact and cell spreading in cultured epithelial cells. *J. Cell Biol.* **99**, 1424-1433.

Colin, P. G. (1856). *Traité de Physiologie Comparée des Animaux Domestiques*. Paris: J. B. Ballière.

Cunningham, J. G. (2002). *Veterinary Physiology*, 296 pp. Philadelphia, PA: W. B. Saunders Company.

Danielli, J. F., Hitchcock, W. S., Marshal, R. A. and Phillipson, A. T. (1945). The mechanism of absorption from the rumen as exemplified by the behaviour of acetic, propionic, and butyric acids. *J. Exp. Biol.* **22**, 75-84.

Decker, P., Gärtner, K., Hörnicke, H. and Hill, H. (1961). Fortlaufende Messungen von Harnstoffbildung und Harnstoffrückfluss in den Pansen in Abhängigkeit vom Harnfluss mit Hilfe von ^{14}C-Harnstoff bei Ziegen. *Pflugers Arch.* **274**, 289-294.

Dobson, A. (1959). Active transport through the epithelium of the reticulo-rumen sac. *J. Physiol.* **146**, 235-251.

Dobson, A. and Phillipson, A. T. (1958). The absorption of chloride ions from the reticulo-rumen sac. *J. Physiol.* **140**, 94-104.

Edrise, B. M., Smith, R. H. and Hewitt, D. (1986). Exchanges of water and certain water-soluble minerals during passage of digesta through the stomach compartments of young ruminating bovines. *Br. J. Nutr.* **55**, 157-168.

Frank, P. G., Hassan, G. S., Rodriguez-Feo, J. A. and Lisanti, M. P. (2007). Caveolae and caveolin-1: novel potential targets for the treatment of cardiovascular disease. *Curr. Pharm. Des.* **13**, 1761-1769.

Galfi, P., Gäbel, G. and Martens, H. (1993). Influences of extracellular matrix components on the growth and differentiation of ruminal epithelial cells in primary culture. *Res. Vet. Sci.* **54**, 102-109.

Graham, C. and Simmons, N. L. (2005). Functional organization of the bovine rumen epithelium. *Am. J. Physiol.* **288**, R173-R181.

Harmeyer, J., Birk, R., Varady, J. and Martens, H. (1973). Kinetics of urea metabolism in sheep maintained on protein-free feed. *Z. Tierphysiol. Tierernähr. Futtermittelkd.* **31**, 239-248.

Henrikson, R. C. and Stacy, B. D. (1971). The barrier to diffusion across ruminal epithelium: a study by electron microscopy using horseradish peroxidase, lanthanum, and ferritin. *J. Ultrastruct. Res.* **34**, 72-82.

Kirschner, N., Bohner, C., Rachow, S. and Brandner, J. M. (2010). Tight junctions: is there a role in dermatology? *Arch. Dermatol. Res.* **302**, 483-493.

Kristensen, N. B. (2005). Splanchnic metabolism of volatile fatty acids in the dairy cow. *J. Anim. Sci.* **80**, 2-9.

Krug, S. M., Fromm, M. and Günzel, D. (2009). Two-path impedance spectroscopy for measuring paracellular and transcellular epithelial resistance. *Biophys. J.* **97**, 2202-2211.

Leonhard-Marek, S., Stumpff, F. and Martens, H. (2010). Transport of cations and anions across forestomach epithelia: conclusions from *in vitro* studies. *Animal* **4**, 1037-1056.

Lioni, M., Brafford, P., Andl, C., Rustgi, A., El-Deiry, W., Herlyn, M. and Smalley, K. S. (2007). Dysregulation of claudin-7 leads to loss of E-cadherin expression and the increased invasion of esophageal squamous cell carcinoma cells. *Am. J. Pathol.* **170**, 709-721.

Martens, H. and Harmeyer, J. (1978). Magnesium transport by isolated rumen epithelium of sheep. *Res. Vet. Sci.* **24**, 161-168.

Martens, H., Gäbel, G. and Strozyk, B. (1991). Mechanism of electrically silent Na and Cl transport across the rumen epithelium of sheep. *Exp. Physiol.* **76**, 103-114.

Masson, M. J. and Philipson, A. T. (1952). The composition of the digesta leaving the abomasum of sheep. *J. Physiol.* **116**, 98-111.

McDonald, I. W. (1948). The absorption of ammonia from the rumen of the sheep. *Biochem. J.* **42**, 584-587.

Milatz, S., Krug, S. M., Rosenthal, R., Günzel, D., Muller, D., Schulzke, J. D., Amasheh, S. and Fromm, M. (2010). Claudin-3 acts as a sealing component of the tight junction for ions of either charge and uncharged solutes. *Biochim. Biophys. Acta* **1798**, 2048-2057.

Mutoh, K. and Wakuri, H. (1989). Early organogenesis of the caprine stomach. *Nippon Juigaku Zasshi* **51**, 474-484.

Phillipson, A. T. and McAnnally, R. A. (1942). Studies on the fate of carbohydrates in the rumen of sheep. *J. Exp. Biol.* **19**, 199.

Plaizier, J. C., Krause, D. O., Gozho, G. N. and McBride, B. W. (2008). Subacute ruminal acidosis in dairy cows: the physiological causes, incidence and consequences. *Vet. J.* **176**, 21-31.

Schmitz, H., Rokos, K., Florian, P., Gitter, A. H., Fromm, M., Scholz, P., Ullrich, R., Zeitz, M., Pauli, G. and Schulzke, J. D. (2002). Supernatants of HIV-infected immune cells affect the barrier function of human HT-29/B6 intestinal epithelial cells. *AIDS* **16**, 983-991.

Schnorr, B. and Wille, K. H. (1972). Zonulae occludentes in the goat ruminal epithelium. *Z. Zellforsch. Mikrosk. Anat.* **124**, 39-43.

Scott, A., Gardner, I. C., Fulton, D. R. and McInroy, G. B. (1972). Tight junctions in the stratum basale of the ruminal epithelium. *Z. Zellforschung.* **131**, 199-203.

Shen, L., Weber, C. R., Raleigh, D. R., Yu, D. and Turner, J. R. (2010). Tight junction pore and leak pathways: a dynamic duo. *Annu. Rev. Physiol.* **73**, 283-309.

Sperber, I. and Hyden, S. (1952). Transport of chloride through the ruminal mucosa. *Nature* **169**, 587.

Stevens, C. E. and Stettler, B. K. (1966). Transport of fatty acid mixtures across rumen epithelium. *Am. J. Physiol.* **211**, 264-271.

Stumpff, F., Martens, H., Bilk, S., Aschenbach, J. R. and Gäbel, G. (2009). Cultured ruminal epithelial cells express a large-conductance channel permeable to chloride, bicarbonate, and acetate. *Pflugers Arch.* **457**, 1003-1022.

van der Velden, L. A., Manni, J. J., Ramaekers, F. C. and Kuijpers, W. (1999). Expression of intermediate filament proteins in benign lesions of the oral mucosa. *Eur. Arch. Otorhinolaryngol.* **256**, 514-519.

Van Itallie, C. M. and Anderson, J. M. (2006). Claudins and epithelial paracellular transport. *Annu. Rev. Physiol.* **68**, 403-429.

Table S1. Primers used for the identification of omasal claudins

Primer no.	Primer name	Sequence
I	bov CLDN1 for	ATGGCCAACGCGGGGTTGCA
	bov CLDN1 rev	TCACACATAGTCTTTCCCACTGGAAG
II	bov CLDN2 for	ATGGCCTCTCTTGGCCTCCAGCTT
	bov CLDN2 rev	TCACACATACCCCGTCAGGCTGTAG
III	bov CLDN3 for	ATGTCCATGGGCCTGGAGATCGC
	bov CLDN3 rev	TCAGACGTAGTCCTTGCGGTCGTAG
IV	bov CLDN4 for	ATGGCTTCCATGGGGCTGCAGGT
	bov CLDN4 rev	TTAGACGTAGTTGCTGGCTGGGGC
V	bov CLDN5 for	ATGGGGTCGGCGGCGCTGGAGATTC
	bov CLDN5 rev	CAGACGTAGTTCTTCTTGTCATAGTCCGGT
VI	bov CLDN7 for	ATGGCCAATTCGGGCCTGCAGCTGC
	bov CLDN7 rev	TCACACATACTCTTTGGCAGAGTTGG
VII	bov CLDN8 for	ATGGCTACCTACGCCCTGCAAA
	bov CLDN8 rev	CTACACGTACTGACTTTTGGAGTAC
VIII	bov CLDN10-1 for	ATGGCGAGCACGGCGTCGG
	bov CLDN10-2 for	ATGTCCAGGGCTCAGATCTCGG
	bov CLDN10 rev	TTAGACGTATGCGTTTTTGTCAAACTGTTTTGAAG
IX	bov CLDN11 for	ATGGTGGCCACATGCTTGCAG
	bov CLDN11 rev	TTATACATGGGCACTCTTGGCATGA
X	bov CLDN12 for	ATGGGCTGTCGGGATGTCCAC
	bov CLDN12 rev	TTAGGTGGTGTGGGAAACTACTGG
A	bov Cldn1m for	AGCGCGGGCGCCCGAGCGAGTCATG
	bov Cldn1m rev	CTTGTTGGTTCCAACAGGATTGTCAGCTTTCGCTTCTGTG
B	bov Cldn2m for	CTAAGCCGCGTGTGCTGAGAGGTCTACCATG
	bov Cldn2m rev	CACCCCCAGCTCTGGCCCCTGGTTCT
C	bov Cldn3m for	AGCCGGCTTTGGCGCGGCAGCCATG
	bov Cldn3m rev	GGAGTGGTCGGGGCTTCCCGCGGTC
D	bov Cldn4m for	TCGCCTCTTCGCCGACGCTGAGCCATG
	bov Cldn4m rev	CAGTGAGCTCAGTCCAGGGAGAAACAAAGATGAAAGG
E	bov Cldn7m for	GCGCCCCCCGTCTATTCTGAAGGCGGAA
	bov Cldn7m rev	GGTTGGGGCAGGGGCGTCCCAACTCA
F	bov Cldn1 middle for	GGGACTAATAGCCATCTTTGTGGCC
	bov Cldn4 middle for	GGCGGCCCGTGCCCTCATCGTCATCTGTA
	bov Cldn7 middle for	ACGACTCGGTGCTCTCCCTGCCGGC

Primers I–X were used for initial screening, primers A–E were used for the cloning and sequencing of sheep omasal claudins, and primer F was used for verification of sequencing. All primers are based on bovine sequences published in the NCBI nucleotide database; however, primers A–E are not within the open reading frame to obtain the genuine sheep sequence.

Table S2. Sequences for sheep claudin-1, -4 and -7 mRNA [complete coding sequences (CDSs)] and protein

HM117762.1 **Claudin-1**

>Seq1 [organism=Ovis aries] Ovis aries claudin 1 (CLDN1) mRNA, complete CDS

ATGGCCAACGCGGGGTTGCAGCTGCTGGGCTTCATCCTGGCGTTTCTGGGCTGGATCGGCTCCATCGTCAGCACGGCGCTGCCCCAGTGGAAGGTTT
ACTCCTATGCTAGTGACAACATCGTGACGGCCCAGGCCATCTACGAGGGGCTGTGGATGTCGTGCGTGTCGCAGAGCACCGGGCAGATCCAGTGCAA
AGTCTTCGACTCCTTGCTGAATCTGAACAGCACTCTGCAAGCAACCCGTGCCTTGATGGTGATCGGCATCCTGCTGGGACTAATAGCCATCTTTGTGGC
CACCCTTGGCATGAAGTGTATGAAGTGCATGGAAGACGACGAGGCACAGAAGATGCGGATGGCTGTCTTTGGGGGCGTGATCTTTCTTATTTCAGGTCT
GGCTGTTTTGGTTGCCACAGCATGGTATGGCAATAGAATTGTTCAAGAAtTCTATGACCCCATGACCCCGGTcAATGCCAGGTATGAATTTGGTCAGGCT
CTCTTCATtGGCTGGGcTGcTGCTTCTCTCTGCCTTCTGggAGGCGCCCTGCTGTGCTGCTCCTGtCcCCGGAAAACAACATCTTACCCAACACCCAGGCC
CTATCCCAAGCCAGCACCTTCCAGTGGGAAAGACtATGTGTGA

>Seq1 Ovis aries claudin 1

MANAGLQLLGFILAFLGWIGSIVSTALPQWKVYSYASDNIVTAQAIYEGLWMSCVSQSTGQIQCKVFDSLLNLNSTLQATRALMVIGILLGLIAIFVATLGMKCMK
CMEDDEAQKMRMAVFGGVIFLISGLAVLVATAWYGNRIVQEFYDPMTPVNARYEFGQALFIGWAAASLCLLGGALLCCSCPRKTTSYPTPRPYPKPAPSSGKD
YV

HM117763.1 **Claudin-4**

>Seq2 [organism=Ovis aries] Ovis aries claudin 4 (CLDN4) mRNA, complete CDS

ATGGCTTCCATGGGGCTGCAGGTGATGGGCATCGCGCTGGCCGTGCTGGGCTGGCTGGGCGCCATCCTGAGCTGCGCGCTGCCCATGTGGCGGGTG
ACGGCCTTCATCGGCAGCAACATCGTCACGTCGCAGACCATCTGGGAGGGCCTGTGGATGAACTGCGTGGTGCAGAGCACCGGCCAGATGCAGTGCA
AGGTGTACGACTCGCTGCTGGCGCTGCCGCAGGACCTGCAGGCGGCCCGCGCCCTCATCGTCATCTGTATCATCCTGGCCGTGTTTGGCGTGCTGTT
GTCGGTGGTGGGCGGCAAGTGCACCAACTGCGTGGATGATGAGAGCCCCAAGGCCAAGATTATGATCGTGGCCGGCGTGGTGTTCCTGCTGGCCGG
CCTGCTGGTGATGGTGCCCGTGTCCTGGACGGCTAACAACGTCATCCGTGACTTCTACAACCCCCTGGTAGCCTCGGGCCAGAAGCGGGAGATGGGG
GCCTCGCTCTACGTGGGCTGGGCCGCCGCTGGCTTGCTGATGCTTGGGGGGACCCTGCTCTGCTTCAACTGCCCGCCACGCAACAACAAGCCCTACT
CCGCTAAGTACTCCGCCGCCCGCTCCGCCCCAGCCAGCAACTATGTCTAA

>Seq2 Ovis aries claudin 4

MASMGLQVMGIALAVLGWLGAILSCALPMWRVTAFIGSNIVTSQTIWEGLWMNCVVQSTGQMQCKVYDSLLALPQDLQAARALIVICIILAVFGVLLSVVGGKCT
NCVDDESPKAKIMIVAGVVFLLAGLLVMVPVSWTANNVIRDFYNPLVASGQKREMGASLYVGWAAAGLLMLGGTLLCFNCPPRNNKPYSAKYSAARSAPASN
YV

HM142819.1 **Claudin-7**

>Seq3 [organism=Ovis aries] Ovis aries claudin 7 (CLDN7) mRNA, complete CDS

ATGGCCAATTCGGGCCTGCAGCTGCTGGGCTTTTCCATGGCTCTGGTGGGCTGGGTGGGCCTGGTGGCATGCACCGCCATCCCGCAGTGGCAGATGA
GCTCGTACGCTGGCGACAATATCATCACCGCCCAGGCCATGTACAAGGGGCTGTGGATGGACTGCGTCACGCAGAGCACCGGCATGATGAGCTGCAA
AATGTACGACTCGGTGCTCTCCCTGCCGGCGGCCTTGCAGGCCACTCGAGCCCTAATGGTGGTTTCCCTGGTGCTGGGCTTCCTGGCCaCATTCGTGG
CCaCGATGGGCATGAAGTGTACAAACTGTGGGGGAGACGACAAAGTGAAGAAGGCCCGGATAGCCATGACGGGAGGCATCATTTTCATCTTGGCAGGT
CTTGCTGCCTTGATAGCTTGCTCCTGGTACGGCCATCAGATTGTCTCAGATTTCTATAACCCGTTGGTCCCCATGAATGTTAAGTATGAATTTGGTCCTG
CCATCTTCATTGGCTGgGCAgGGTCTGCTCTGATCATCCTGGGAGGTGCGCTGCTCTCTTGCTCCTGTCCTGGGAGTGAGAGCAAAGCTGGATACCGTG
CACCTCGCTCCTACCCTAAGCCCAACTCTGCCAAGGAGTATGTGTGA

>Seq3 Ovis aries claudin 7

MANSGLQLLGFSMALVGWVGLVACTAIPQWQMSSYAGDNIITAQAMYKGLWMDCVTQSTGMMSCKMYDSVLSLPAALQATRALMVVSLVLGFLATFVATMG
MKCTNCGGDDKVKKARIAMTGGIIFILAGLAALIACSWYGHQIVSDFYNPLVPMNVKYEFGPAIFIGWAGSALIILGGALLSCSCPGSESKAGYRAPRSYPKPNSA
KEYV

Differences compared with cattle (*Bos taurus*) are marked in yellow.